Am J Cancer Res 2023;13(5):1698-1717
www.ajcr.us /ISSN:2156-6976/ajcr0150612

Original Article

A human pan-cancer system analysis of heat shock protein family A member 5

Chao Deng[1,2], Siming Gong[1,2], Lizhen Lin[3], Juyu Tang[1,2], Xiaoyang Pang[1], Panfeng Wu[1,2]

[1]Department of Orthopedics, Xiangya Hospital, Central South University, Changsha, Hunan, China; [2]National Clinical Research Center for Geriatric Disorders, Xiangya Hospital, Central South University, Changsha, Hunan, China; [3]Department of Endocrinology, Xiangya Hospital, Central South University, Changsha, Hunan, China

Received April 7, 2023; Accepted April 27, 2023; Epub May 15, 2023; Published May 30, 2023

Abstract: Heat shock protein family A member 5 (HSPA5) plays a pivotal role in the endoplasmic reticulum (ER) stress response and unfolded protein response (UPR), both of which are crucial for protein folding, assembly, and quality control within cells. In response to ER stress, HSPA5 becomes overexpressed to preserve cellular homeostasis. A previous study revealed a robust association between HSPA5 expression and various cancers. However, the prognostic function of HSPA5 and its involvement in tumor formation remain largely unknown. In this study, we integrated HSPA5 expression data from databases such as the Clinical Proteomic Tumor Analysis Consortium (CPTAC) and The Cancer Genome Atlas (TCGA) to conduct a comprehensive pan-cancer analysis of HSPA5. Our findings revealed that HSPA5 is overexpressed in various tumor types and is significantly associated with poor prognosis. Additionally, HSPA5 expression is significantly correlated with immune checkpoints, stromal infiltration, and consequent alterations in the immune landscape. Verification was conducted on samples from patients with various tumor types, including breast and liver cancers. Additionally, we also performed verification in vitro. In conclusion, HSPA5 may offer a potential target for cancer treatment.

Keywords: HSPA5, pan-cancer, prognosis, enrichment analysis, immune infiltration, Immune checkpoint inhibitor

Introduction

HSPA5, alternatively referred to as glucose-regulated protein 78 kDa (GRP78) or binding immunoglobulin Protein (BiP), is a constituent of the heat shock protein 70 (HSP70) family and functions as a vital molecular chaperone in the endoplasmic reticulum (ER). This protein is implicated in various critical cellular processes. As an ER chaperone, HSPA5 assists in the folding and assembly of newly formed proteins entering the secretory pathway, thereby ensuring their proper conformation and preventing aggregation. Moreover, HSPA5 plays a role in protein degradation by directing misfolded proteins toward ER-associated degradation [1, 2]. Owing to its participation in numerous cellular functions, HSPA5 is also associated with a range of pathological conditions, including autoimmune disorders, cancer, and neurodegenerative diseases [3-7].

Under normal physiological conditions, HSPA5 expression is maintained at low levels. Nevertheless, its expression increases in response to ER stress, as observed in situations involving nutrient deprivation, hypoxia, and accumulation of unfolded proteins [1]. Recently, an association between HSPA5 and cancer has been reported. Through epidermal growth factor receptor (EGFR) mutations, HSPA5 has been linked to the promotion of lung carcinoma growth [8]. Moreover, HSPA5 overexpression has been correlated with enhanced cell metastasis, proliferation, migration, angiogenesis, invasion, and aggressive tumor phenotypes in breast cancer [8-11]. Recent studies have also revealed a connection between HSPA5 and the emergence of resistance to anti-cancer therapies, including targeted therapy and chemotherapy, in hepatocellular carcinoma cells [12-15]. Additionally, elevated HSPA5 expression levels have been found to correlate with poor clinical outcomes in osteosarcoma patients,

including reduced overall survival (OS) and increased recurrence rates [16-19].

Various studies have focused on specific cancer types, including lower-grade glioma (LGG) of the brain and thyroid carcinoma (THCA). However, conducting a comprehensive pan-cancer analysis of HSPA5 is essential for unveiling its roles. In this study, we performed a pan-cancer analysis of HSPA5 based on the comprehensive examination of various databases, including the Clinical Proteomic Tumor Analysis Consortium (CPTAC) and The Cancer Genome Atlas (TCGA). We investigated multiple facets of HSPA5 across diverse cancer types, including its modifications, transcriptional and translational expression, prognostic implications, and immune-associated assessments. To further explore the possible function of HSPA5 in human cancers, gene enrichment analyses encompassing HSPA5-related and HSPA5-interacting genes were conducted. Additionally, the expression of HSPA5 was validated using samples collected from 12 patients, and the knock down of HSPA5 was found to impact the proliferation, migration, and invasion capabilities of Hep3B cells. Our results lay the groundwork for additional research by emphasizing the possible roles and unique mechanisms of HSPA5 in human cancers.

Materials and methods

Gene alteration analysis and gene expression at transcription and translation level

An examination of HSPA5 genetic alterations was performed using the cBioPortal tool [20]. Data pertaining to HSPA5 alterations across diverse tumor types were collected using the "TCGA Pan-Cancer Atlas Studies" module. Information on HSPA5 mutation sites was obtained from the cBioPortal.

The "Gene DE" module of the Tumor Immune Estimation Resource version 2 (TIMER2) was entered using "HSPA5" [21]. Using TCGA, difference of HSPA5 expression between cancers and corresponding normal tissues across different cancers or specific tumor subtypes were assessed [22]. The results from the TCGA cohort were selected for validation in breast invasive carcinoma (BRCA), liver hepatocellular carcinoma (LIHC), and colon adenocarcinoma (COAD) [23]. The UALCAN website, which offers protein expression data, was used to investigate translational changes in HSPA5 expression between normal and cancer tissues [24]. Six tumor types were examined: uterine corpus endometrial carcinoma (UCEC), ovarian cancer, colon cancer, head and neck squamous cell carcinoma (HNSC), and Kidney renal cell carcinoma (KIRC). The translational expression of HSPA5 in various organs, single cells, and tumors was investigated using data from the Human Protein Atlas (HPA) cohort. The HPA database contains immunohistochemical staining data for HSPA5 across multiple tumor types.

Survival analysis

R software (version 3.6.3) was utilized to examine the relationship between HSPA5 expression and prognosis in various cancers. The optimal cut-off was determined individually for each cancer type. A survival heatmap and Kaplan-Meier survival curves were generated to visualize the results. To gain a more comprehensive understanding of the association between HSPA5 expression and prognostic outcomes in different cancer types, survival data were obtained from TCGA [25]. Moreover, using the R packages "survminer" and "survival", disease-specific survival (DSS) and progression-free interval (PFI) analyses were conducted, based on TCGA data.

Related gene network construction

The protein-protein interaction (PPI) network of HSPA5 was built using STRING, which identified 50 known or projected HSPA5-interacting proteins. Additionally, the top 100 HSPA5-correlated genes were determined using data from TCGA cohort using the GEPIA2 tool. Using a combination of HSPA5-interacting genes and HSPA5-correlated genes, Kyoto Encyclopedia of Genes and Genomes (KEGG) pathway analysis and Gene Ontology (GO) enrichment analysis comprising biological processes, cellular components, and molecular functions were performed.

Gene set enrichment analysis of HSPA5 in pan-cancer

Gene set enrichment analysis (GSEA) was performed on high- and low-expression groups

using the mean expression value of HSPA5 across 33 cancer types in TCGA to explore biological and cancer-associated signaling pathways. The GSEA was conducted using the "clusterProfiler" R package.

Immune-related analysis

In all tumors, HSPA5 expression was standardized and transformed using the log2(x+1) formula. Immunological, estimation, and stromal scores for each cancer type were acquired using the SangerBox online platform [26]. Furthermore, the relationships between 60 immunological checkpoint (ICP) genes and HSPA5 expression were investigated. The TIMER2 software was used to explore the correlation between HSPA5 expression and cancer-associated fibroblasts (CAFs) across various cancer types. Cellular heterogeneity of HSPA5 expression in various cancers was conducted using Cancer Single-cell Expression Map [27].

Immunohistochemical staining

12 Patients who received surgical intervention and were diagnosed with breast cancer, stomach cancer, liver cancer or other disease at Xiangya hospital of Central South University contributed tumor tissue and corresponding normal tissue samples for this study. The ethics committee of Xiangya Hospital of Central South University approved all related procedures, and the study was conducted in compliance with the Declaration of Helsinki.

Tissues were prepared following conventional procedures involving paraffin embedding. These tissues were sectioned into 3 μm thick slices and consecutively cut for hematoxylin and eosin (H&E) staining. The tissue sections were heated in Tris-EDTA buffer (pH 9.0) and maintained at a temperature just below the boiling point for 20 min to retrieve antigen immunoreactivities for immunohistochemical staining (IHC). To stop the endogenous peroxidase activity, soaked tissue slices were incubated in 3.0% hydrogen peroxide for 10 min at room temperature. The tissue sections were incubated with antibodies against HSPA5 (1:150 dilution; Abmayt, Shanghai, China) and PL-L1 (1:400 dilution; Proteintech) for 1 h at room temperature. The sections were incubated using a Max-Vision HRP-Polymer anti-Rabbit IHC Kit (MXB Biotechnologies, Fuzhou, China) for 30 min. Tissue slices were treated with DAB working solution (MXB Biotechnologies, Fuzhou, China) for color development. An upright Olympus microscope was used to study the tissue slices. Based on the staining intensity and proportion of positive cells, two pathologists who were blinded to the identities of the samples independently evaluated the staining results. Intensity scores were 0 (negative), 1 (weakly positive), 2 (moderately positive), and 3 (strongly positive). The proportions of positive cells were: 0 (0%), 1 (1%-25%), 2 (26%-50%), and 3 (> 50%). The intensity score and proportion of positive cells were added to obtain the IHC score [28].

Cell culture

The human hepatocellular carcinoma cell line Hep3B was obtained from the Xiangya Cell Repository. Cells were cultured in Dulbecco's Modified Eagle's Medium (DMEM; BasalMedia, China) supplemented with antibiotics and 10% fetal bovine serum (Gibco, USA) under 5% CO_2 and 37°C conditions. Small interfering RNAs (siRNAs) targeting HSPA5 and the empty vector (si-NC) were synthesized by GenePharma (Shanghai, China). Cell transfection was performed using Lipofectamine® 3000 (Invitrogen/Thermo Fisher Scientific, USA) according to the manufacturer's instructions.

CCK-8 assay

Cell proliferation activity was assessed using the CCK-8 assay kit (Beyotime, China). After transfection, cells were cultured for 24 hours and then seeded in several 96-well plates at a density of 2,000 cells per well. Following cell adherence, 10 μl of CCK-8 reagent (Beyotime, China) was added to each well after 24, 48, and 72 hours of incubation. One hour later, the absorbance values of each well were measured at 450 nm using a microplate reader.

Transwell assay

The invasiveness of the cells was assessed using a Transwell assay. A total of 5 × 10^4 transfected Hep3B cells were seeded in the upper chamber and incubated in 5% serum medium, while the lower chamber was incubated in 10% serum medium. After 24 hours of incubation, the matrix gel was removed from the upper chamber with a cotton swab, and the

Figure 1. HSPA5 mutation in specific TCGA tumors. A. Types and frequencies of alterations. B. Genetic alterations of HSPA5, including types, locations, and frequencies.

cells on the chamber membrane were fixed with 4% paraformaldehyde and stained with crystal violet. Five random fields of view were counted for each chamber.

Wound healing assay

The migration ability of the cells was assessed using a wound healing assay. Transfected cells were evenly seeded in 12-well plates and cultured until 80% confluence was reached. A 200 μl pipette tip was used to create horizontal and vertical scratch lines, and the culture medium was replaced to remove detached cells. At 0 hour and 36 hours post-scratch, four fields of view were captured at the top, bottom, left, and right sides of each cross-junction for a total of 4 fields per well.

Results

Gene alteration Information analysis

The cBioPortal tool revealed that HSPA5 genetic variation was notably diverse and frequent, with mutation rates of 4.73%, 1%, 0.67%, and 0.39% in UCEC, COAD, acute myeloid leukemia (AML), and testicular germ cell tumors (TGCT), respectively (**Figure 1A**). These tumors display various types of mutations. In contrast, kidney chromophobe (KICH), esophageal adenocarcinoma (EAC), LGG, and kidney renal papillary cell carcinoma (KIRP) showed only a single amplification type, with frequencies of 1.54%, 1.1%, 0.97%, and 0.35%, respectively. Other tumors exhibited a combination of two or more alteration types. Across various tumors, 102 variants of uncertain significance (VUS) in HSPA5 were identified (**Figure 1B**). The transcriptional expressions of HSPA5 in the TCGA cohort, along with the various copy numbers and mutations, are presented in Supplementary Figure 1.

Gene expression analysis

Data from the GTEx, Human Protein Atlas (HPA), and Functional Annotation of Mammalian Genome 5 (FANTOM5) cohorts were used to compare HSPA5 expression in various healthy organs, single cell types, and tumors. Among normal tissues, bone marrow exhibited

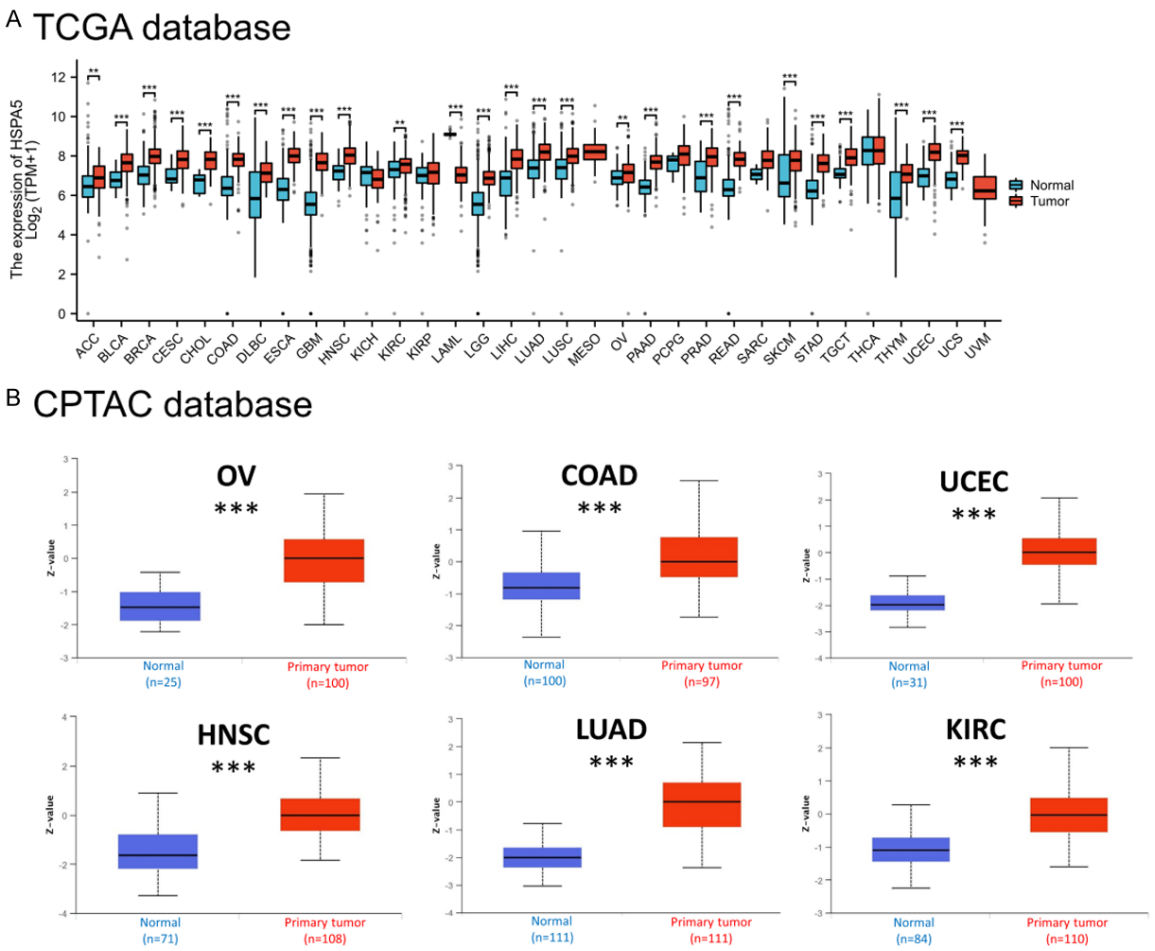

Figure 2. Expression of HSPA5 in various tumors. A. Level of HSPA5 expression in various tumors or specific cancer subtypes. "N" stands for "normal", while "T" stands for "tumor tissue". B. Comparison of total HSPA5 protein expression in tumor tissue and corresponding normal tissue, as revealed by the CPTAC dataset. *P < 0.05; **P < 0.01; ***P < 0.001.

the highest HSPA5 expression; however, there was less RNA tissue specificity (Supplementary Figure 2). In single-cell RNA and RNA cancer classification analyses, HSPA5 expression exhibited limited cell-type specificity and weak cancer specificity (Supplementary Figure 2).

Using TCGA and GTEx databases, the transcriptional expressions of HSPA5 in diverse tumor types were examined. Among 33 common tumor types, HSPA5 was predominantly expressed in 26 tumors compared with the corresponding normal tissues (**Figure 2A**). However, HSPA5 expression was more prevalent in healthy tissues than in acute myeloid leukemia (LAML) tissues (P=0.001). Similarly, in KICH, KIRP, Sarcoma (SARC), and THCA, HSPA5 expression was comparable between normal and malignant tissues. Ovarian serous cystadenocarcinoma (OV), COAD, UCEC, HNSC, lung adenocarcinoma (LUAD), and Kidney renal clear cell carcinoma (KIRC) were among the cancers in which HSPA5 protein expression was markedly elevated in tumor tissues relative to their respective normal tissues (**Figure 2B**). **Figure 3** illustrates the immunohistochemical staining of HSPA5 expression in BRCA, LIHC, and COAD derived from the HPA database.

Survival analysis

Using data from TCGA, two groups were formed based on higher and lower HSPA5 expression levels. The relationship between HSPA5 expression and patient prognosis has been examined in various cancer types. Patients overexpressing HSPA5 in cancers such as BRCA, cervical squamous cell carcinoma, endocervical adeno-

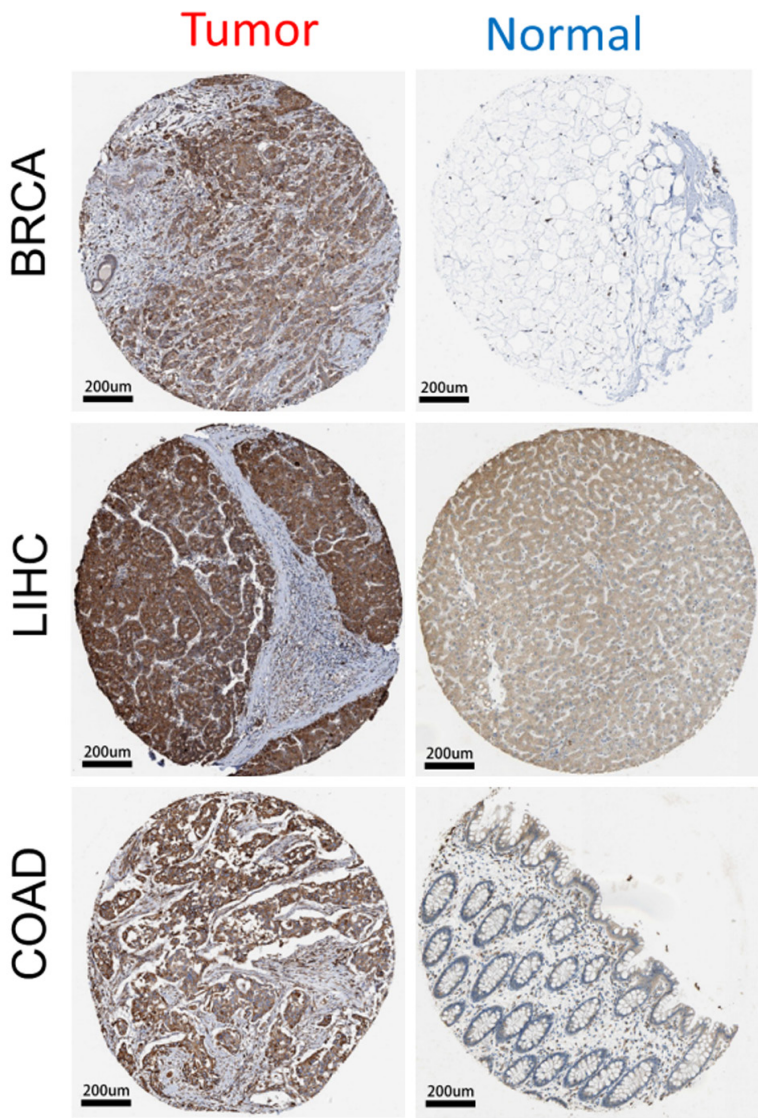

Figure 3. Three tumor types (COAD, LIHC, and BRCA) exhibiting distinct levels of HSPA5 expression at the translational level when compared with their corresponding normal tissues (colon, liver, and breast). Scale bar: 200 μm.

carcinoma (CESC), glioblastoma multiforme (GBM), HNSC, KIRP, LGG, LIHC, LUAD, SARC, and uveal melanoma (UVM) exhibited relatively low OS (**Figure 4**, $P < 0.05$). Patients with ACC, BLCA, CESC, esophageal carcinoma (ESCA), GBM, HNSC, KICH, KIRP, LGG, LIHC, lung squamous cell carcinoma (LUSC), pancreatic adenocarcinoma (PAAD), prostate adenocarcinoma (PRAD), SARC, and UVM with high HSPA5 expression demonstrated low DSS (**Figure 4**, all $P < 0.05$). High HSPA5 expression was associated with PFI in ACC, BLCA, CESC, lymphoid neoplasm diffuse large B-cell lymphoma (DLBC), HNSC, KICH, kidney renal clear cell carcinoma (KIRC), KIRP, LGG, LUSC, PAAD, SARC, and UVM (**Figure 4**, $P < 0.05$). The Kaplan-Meier curves for OS, DSS, and PFI for four representative tumors (HNSC, KIRP, LGG, and SARC) were selected. These findings suggest that HSPA5 may contribute to the progression of various tumors into malignancies and may be a potential predictive biomarker.

Gene enrichment analysis

Using the STRING program, the top 50 HSPA5-interacting proteins were identified and a PPI network was generated (**Figure 5A**). The top 100 genes associated with HSPA5 expression are listed in Supplementary Table 1. HSPA5-interacting and HSPA5-related genes were combined, and KEGG pathway and GO enrichment analyses were conducted. According to KEGG pathway analysis, these genes are involved in processes related to prostate cancer and other cancers. HSPA5 expression is closely associated with atherosclerosis, amyotrophic lateral sclerosis, and other neurodegenerative disorders. HSPA5 is also crucial for protein export and ER-based protein processing (**Figure 5B**).

GO enrichment analysis revealed that HSPA5-interacting and related genes were linked to the biological process (BP) category's functions, such as chaperone-mediated autophagy, response to ER stress, Golgi vesicle transport, response to topologically incorrect proteins, ER to Golgi vesicle-mediated transport, response to unfolded proteins, and response to incorrectly folded proteins (**Figure 5C**). Further analysis indicated a strong connection between the endomembrane system, such as that between the ER protein-containing complex of the cellular component (CC) category and HSPA5 (**Figure 5D**). Molecular function (MF) category analysis

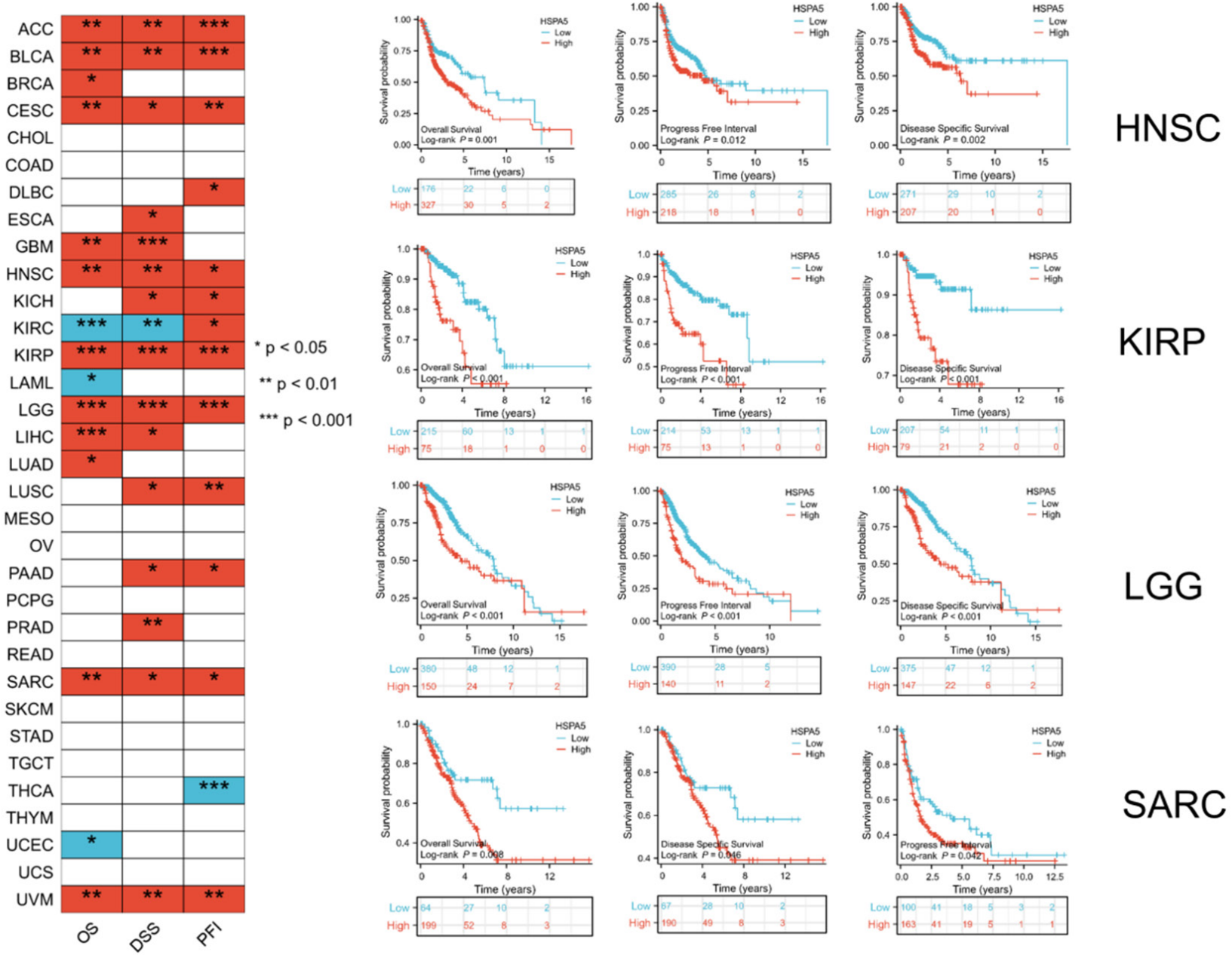

Figure 4. Correlation between HSPA5 gene expression in tumors and survival prognosis in TCGA.

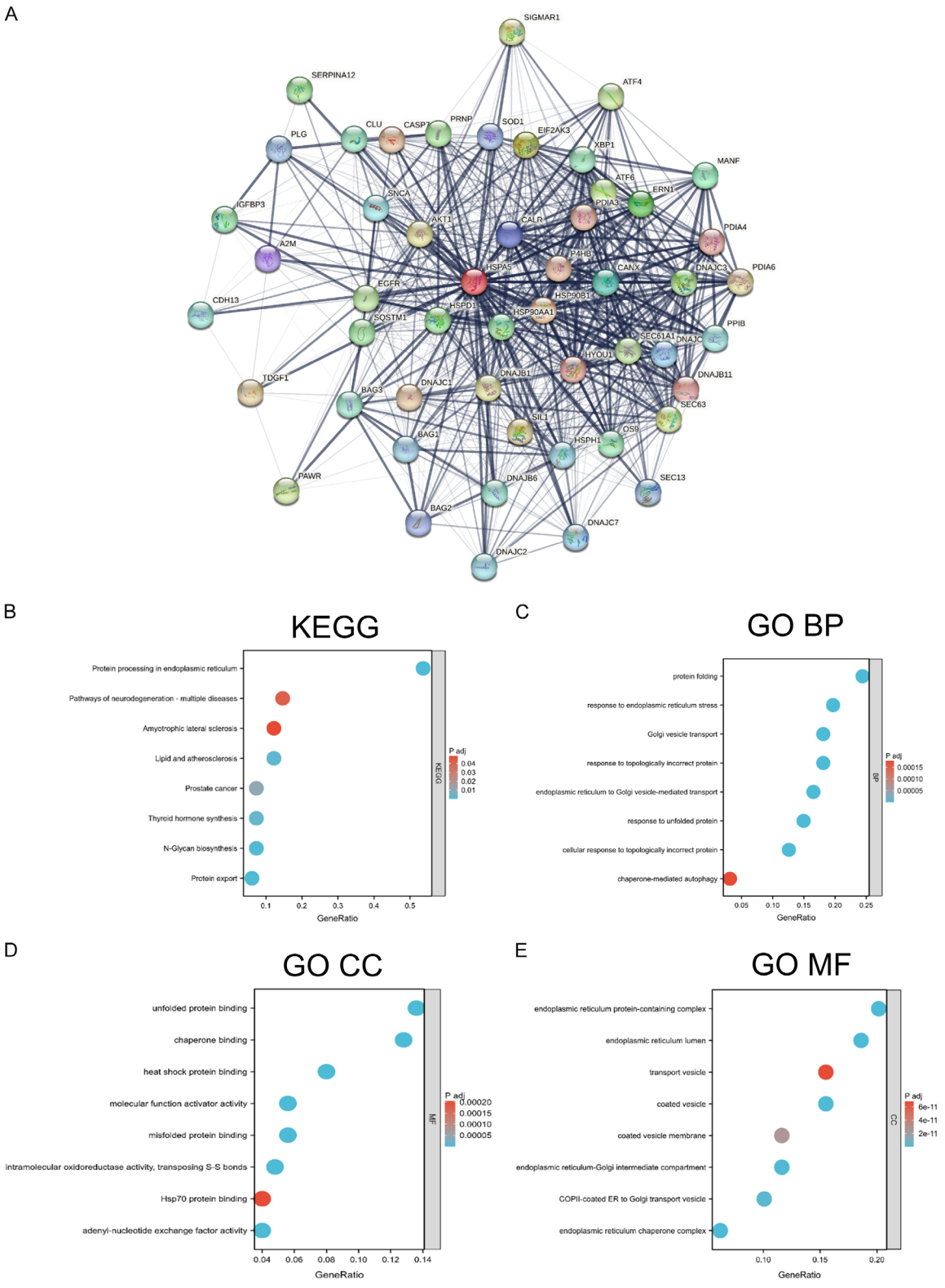

Figure 5. HSPA5-related gene enrichment analysis. A. HSPA5-related proteins identified through experimentation obtained using the STRING tool. B-E. Enrichment analysis of HSPA5 and its most frequent neighbors. HSPA5-binding and interacting genes were employed to perform KEGG pathway and GO enrichment analyses.

demonstrated the relationship between HSPA5 and multiple molecular binding capacities (**Figure 5E**). Additionally, GSEA analysis demonstrated a relationship between the gene expression profile in TCGA cohort patients with high HSPA5 expression and signature cancer-associated genes such as EGFR and BMI1 (**Figure 6**).

Immune-related analysis

The association between HSPA5 expression and CAFs was examined using four algorithms: TIDE, XCELL, EPIC, and MCPCOUNTER. Most algorithms demonstrated similar patterns, len ding credibility to the findings. HSPA5 expression was positively correlated with CAF infiltration in most tumor types, including PRAD, stomach adenocarcinoma (STAD), and THCA, but negatively correlated with CAF infiltration in HNSC, LUSC, LGG, LUAD, COAD, and thymoma (THYM) (**Figure 7A**). **Figure 7B** shows representative scatter plots generated by the algorithms. We investigated the relationship between HSPA5 expression and other immune cells. The immune cell map (Supplementary Figure 3) included 25 different types of immune cells, including classically activated macrophages (M1), alternatively activated macrophages (M2), and active CD8+ T cells. According to the immune map, HSPA5 expression was positively correlated with the immune cells of BLCA, UVM, and BRCA, but negatively correlated with the majority of immune cells in GBM and THCA (Supplementary Figure 3).

The online platform, SangerBox, was used to investigate the relationship between HSPA5 expression and immune infiltration scores. Most of the included tumors displayed significant variations in immune score, stromal score, and ESTIMATE score (**Figure 8A**). In the LGG + GBM group, pan-kidney cohorts (KICH + KIRC + KIRP), BLCA, and HSPA5 exhibited a positive correlation with the ESTIMATE score, stromal score, and immune score. In contrast, it was negatively correlated with LAML, LUAD, PRAD, STAD, stomach and esophageal carcinoma (STES), THCA, and UCEC (p-values < 0.05; **Figure 8B-D**).

HSPA5 was positively associated with the majority of immune checkpoint proteins (ICPs) in various tumors, as evidenced by ICP analyses, including UVM, OV, DLBC, BLCA, the pan-kidney cohort (KICH + KIRC + KIRP), KIPAN, rectal adenocarcinoma (READ), GBM + LGG, COAD, UCEC, THYM, LIHC, KIRC, and KIRP. HSPA5 exhibits a favorable correlation with programmed cell death protein-1 (PDCD1, also known as PD-1), CD152 (cytotoxic T-lymphocyte-associated protein 4, commonly known as CTLA4), and CD274 in a variety of cancers, such as pheochromocytoma and paraganglioma (PCPG), GBM, COAD, and LIHC (also known as PD-L1) (**Figure 9**). Single-cell data revealed that although HSPA5 is expressed to varying degrees in different cell types, it is primarily found in immune and malignant cells. HSPA5 exhibited the highest expression in malignant cells for pancreatic ductal adenocarcinoma (PDAC), non-small cell lung carcinoma (NSCLC), and GBM (Supplementary Figure 4).

Experimental validation

To validate the expression of HSPA5 in human tumor tissues and its relationship with immune checkpoint proteins, we verified bioinformatics predictions. Compared with non-tumor breast and liver tissues, we observed high expression of HSPA5 and PD-L1 in tumor tissues from breast cancer and liver cancer patients (**Figure 10A**). We quantified the results using IHC scoring and found that in BRCA the HSPA5 IHC score was 5.33, while the PD-L1 score was 3.67. In the control group, the HSPA5 score was 1 and the PD-L1 score was 1.67. In the LIHC group, the HSPA5 score was 6.33 and the PD-L1 score was 3.67; in the control group, the HSPA5 score was 2 and the PD-L1 score was 1.67 (**Figure 10B**). Our in vitro experiments demonstrated that knocking down HSPA5 impacted the proliferation, invasion, and migration capabilities of Hep3B cells. In summary, the experimental results obtained are in general consistent with the bioinformatics predictions.

Discussion

HSPA5 is overexpressed in various tumor types, including hepatocellular carcinoma, glioma, breast cancer, and colorectal cancer, among others [29, 30]. This overexpression is associated with increased cell proliferation, metastasis, and apoptosis [31]. Furthermore, high HSPA5 levels are considered indicators of poor prognosis and reduced survival in cancer

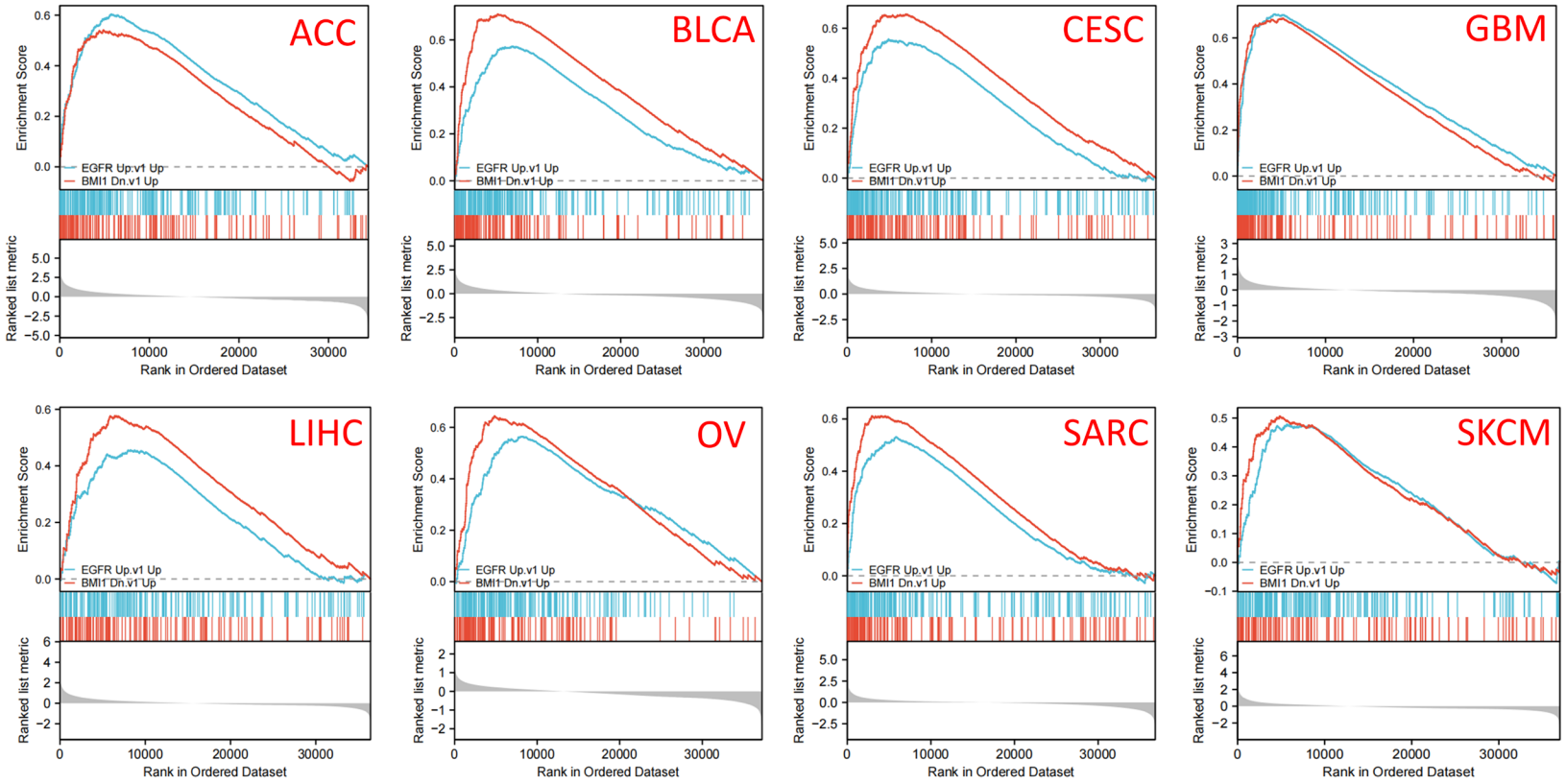

Figure 6. Oncogenic gene set enrichment analysis of HSPA5. Oncogenic signature gene sets enriched in high HSPA5 expression.

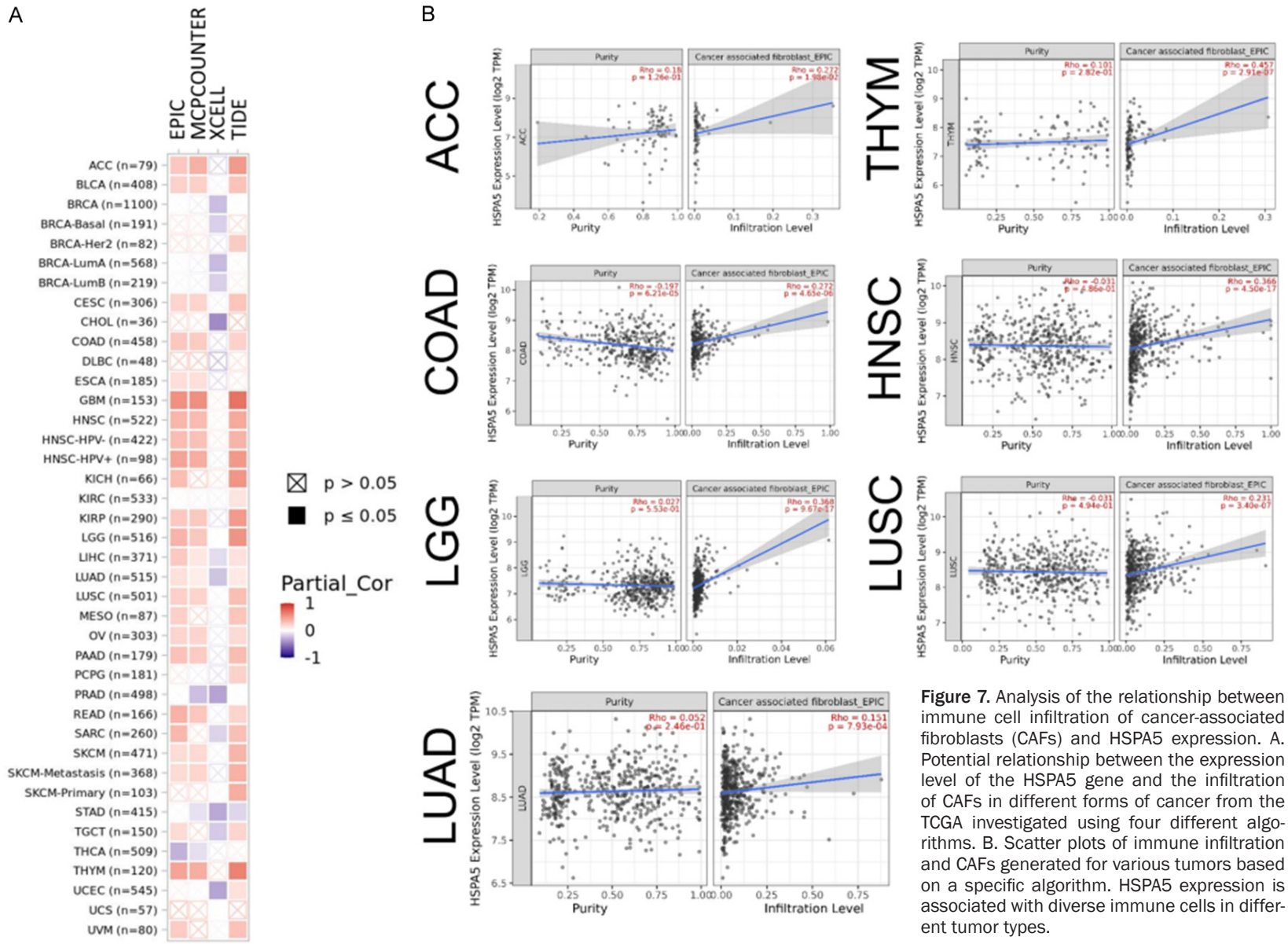

Figure 7. Analysis of the relationship between immune cell infiltration of cancer-associated fibroblasts (CAFs) and HSPA5 expression. A. Potential relationship between the expression level of the HSPA5 gene and the infiltration of CAFs in different forms of cancer from the TCGA investigated using four different algorithms. B. Scatter plots of immune infiltration and CAFs generated for various tumors based on a specific algorithm. HSPA5 expression is associated with diverse immune cells in different tumor types.

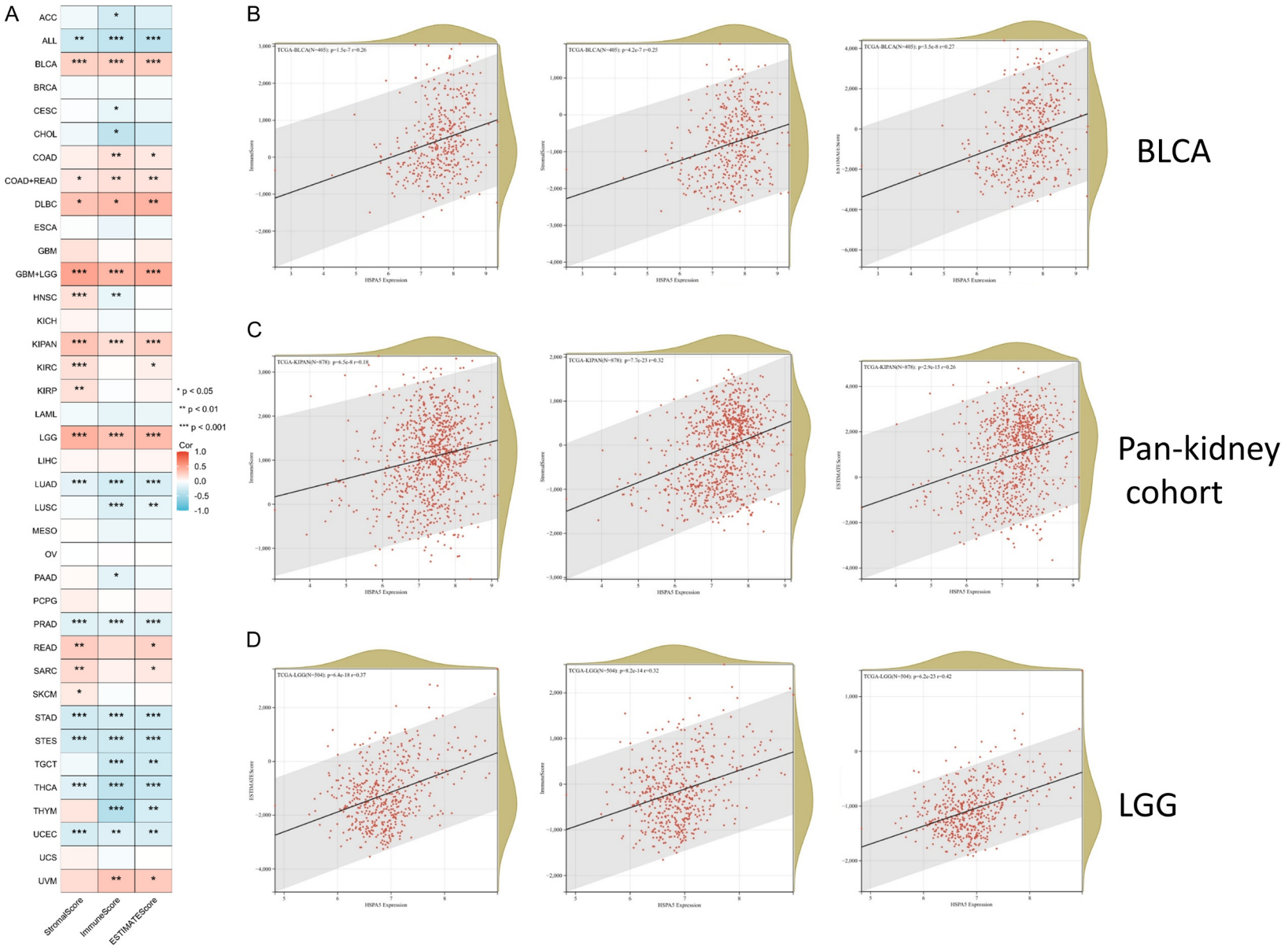

Figure 8. Correlation analysis between HSPA5 expression and immune score, stromal score, and ESTIMATE score. (A) Heatmap displaying correlation across the involved tumors. Three representative tumor types are illustrated: (B) BLCA, (C) Pan-kidney cohort (KICH + KIRC + KIRP), and (D) LGG. *P < 0.05; **P < 0.01; ***P < 0.001.

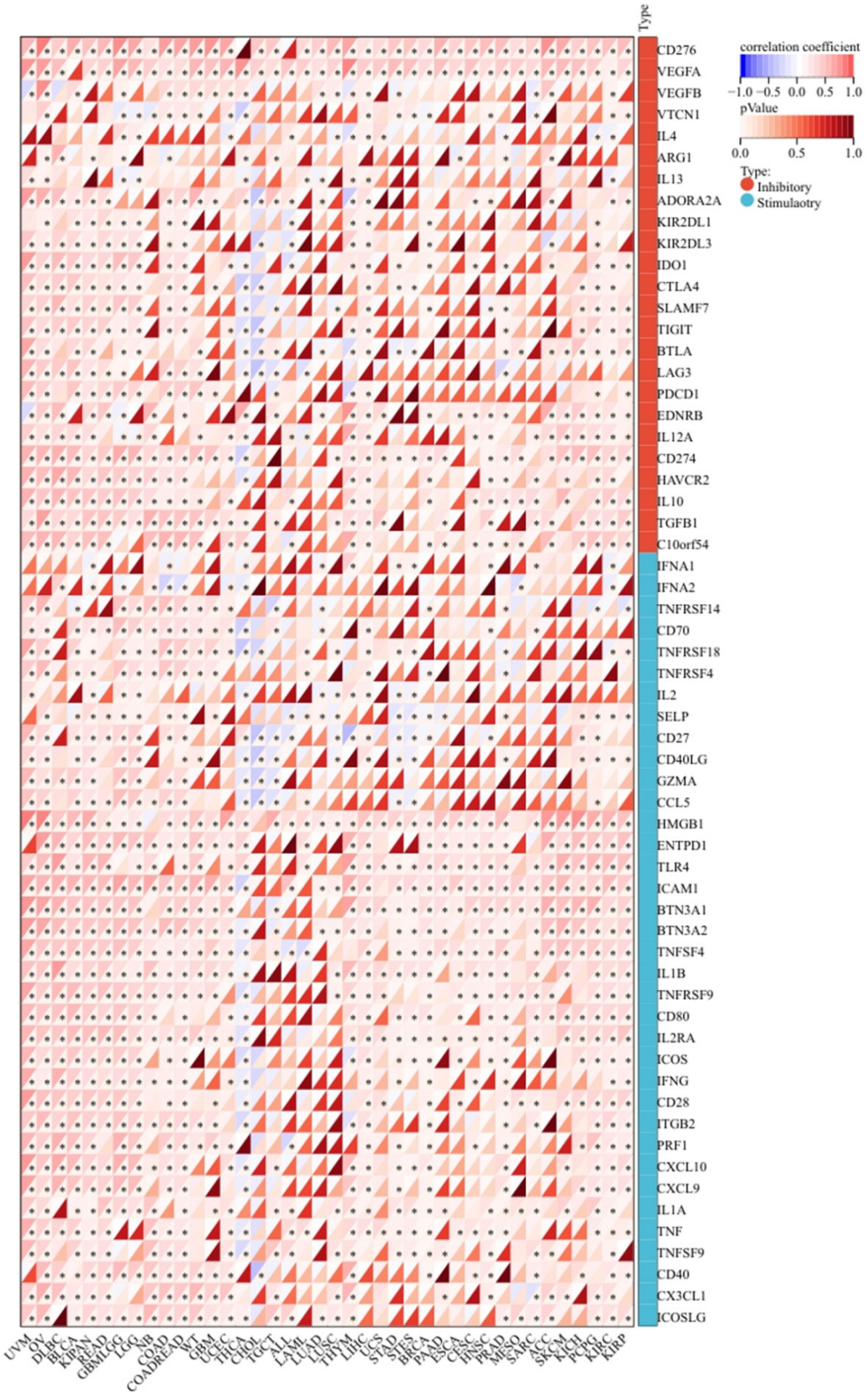

Figure 9. Immune checkpoint (ICP) gene expression and HSPA5 expression correlated in certain cancers. *P < 0.05.

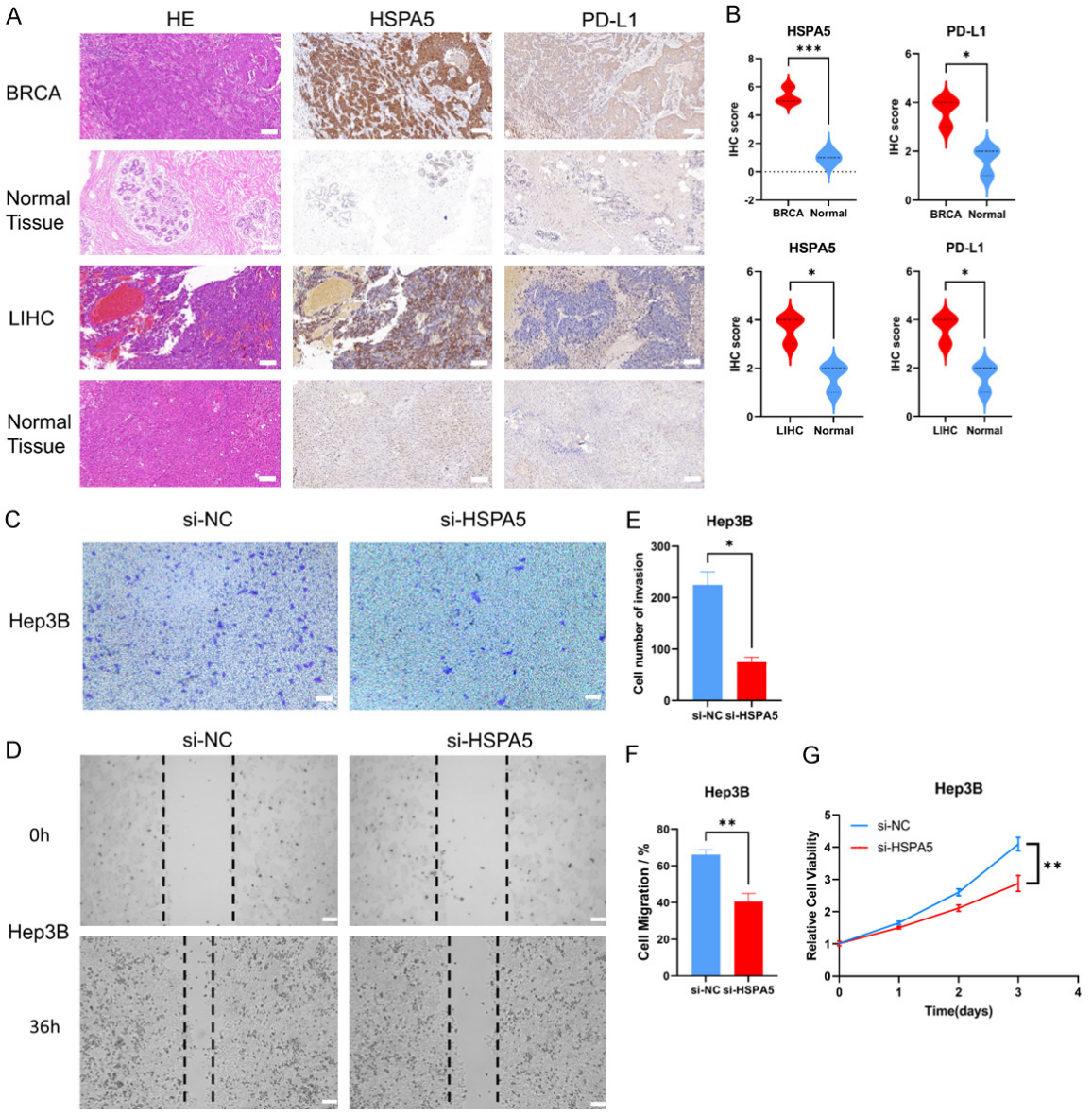

Figure 10. Highly expressed HSPA5 and PD-L1 in BRCA and LIHC. A. IHC staining images of HSPA5 and PD-L1 in BRCA, LIHC, and corresponding normal tissues. Scale bar: 200 μm. B. IHC scores indicating that protein expressions of HSPA5 and LIHC are higher in tumor tissues (n=3). C, E. Transwell experiment showing the effect of HSPA5 knockdown on the invasion of Hep3B cells (n=3). Scale bar: 50 μm. D, F. Wound healing experiment showing the effect of HSPA5 knockdown on the migration of Hep3B cells (n=3). Scale bar: 50 μm. G. Folded line plots showing the effect of HSPA5 knockdown on the proliferation of Hep3B cells (n=3). $^{*}P < 0.05$; $^{*}P < 0.01$; $^{***}P < 0.001$.

patients [32]. Concurrently, HSPA5 is crucial for maintaining ER homeostasis and activating the unfolded protein response (UPR) under stressful conditions such as hypoxia, nutrient deprivation, and oxidative stress, which are commonly encountered in the tumor microenvironment [33]. Moreover, HSPA5 can affect pathways such as the MAPK/ERK and PI3K/AKT pathways, which are important for cell apoptosis [34, 35].

However, despite the significance of HSPA5 in cancer, its role in various human tumors has not been extensively studied. In this study, data from TCGA, GTEx, and CPTAC cohorts facilitated the examination of HSPA5 genetic alterations, gene transcriptional expression of HSPA5, and protein expression of HSPA5 in different cancers. Gene enrichment analysis was performed using a combination of HSPA5-interacting and HSPA5-correlated genes. The

results of this study will facilitate a deeper understanding of the potential mechanisms linking HSPA5 expression with cancer development.

HSPA5 overexpression was observed in the majority of tumors, including BLCA, LGG, CESC, ESCA, and READ, which is consistent with the finding of previous studies [36-38]. HSPA5 genetic variation data indicated that mutations are the primary alterations among different cancers, with the highest mutation rates of 4.73% in UCEC, 2.03% in skin cutaneous melanoma, 1.7% in bladder urothelial carcinoma, and 1.1% in ACC. These gene mutations, amplifications, and deep deletions of HSPA5 in various tumors contribute to the differential expression of mRNA and proteins. HSPA5 expression analysis based on TCGA and GTEx cohorts revealed that 26 types of cancers, including ACC, BLCA, BRCA, and CESC, significantly overexpress HSPA5. Differential expression of HSPA5 may lead to increased cell proliferation, metastasis, angiogenesis, and resistance to apoptosis [31]. Consequently, targeting HSPA5 is a promising approach for treating various types of cancer. Several studies have explored the potential of mutated gene-targeted therapies involving HSPA5. Small molecules and natural compounds such as HA15 and epigallocatechin-3-gallate (EGCG), have shown promising anti-cancer effects by targeting HSPA5 and disrupting its chaperone functions [39, 40]. Moreover, small interfering RNA (siRNA) and short hairpin RNA (shRNA) have been used to suppress HSPA5 expression, leading to decreased tumor growth and increased sensitivity to chemotherapeutic agents [41]. Furthermore, GSEA demonstrated that high HSPA5 expression is associated with oncogenic signatures, including EGFR and BMI1. The roles of EGFR and BMI1 in cancer have been extensively investigated [8].

In summary, our findings support the results of previous studies, indicating that HSPA5 acts as an oncogene. Increased HSPA5 expression has been consistently associated with poor prognosis in various tumor types. In oncology, the main survival endpoints are OS, PFI, and DSS. OS is the most direct and commonly used endpoint in cancer research and is defined as the time from a specific starting point (e.g., treatment initiation or diagnosis) to death from any cause [42]. OS continues to be the gold standard for evaluating the effectiveness of therapeutic interventions as it takes into account all factors influencing patient survival, such as treatment-related side effects, and the natural progression of the disease [43]. In our study, overexpression of HSPA5 was found to be associated with poor prognosis in ACC, BLCA, CESC, HNSC, KIRP, LGG, SARC, and UVM, and correlated with OS, PFI, and DSS. These findings suggest that HSPA5 may serve as a potential biomarker for these tumors and provides valuable information for the development of personalized treatment strategies. However, in kidney tumors, high expression of HSPA5 does not demonstrate a strong statistical significance with OS in KICH, and even presents a favorable prognosis in KIRC, in contrast to KIRP. This result implies that the prognostic utility of HSPA5 could be contingent on the specific subtype of kidney cancer or could potentially be extended to other malignancies.

To further understand the specific mechanisms by which HSPA5 influences tumor progression, we analyzed the interactions of HSPA5 with other genes in cancer. HSPA5 is positively correlated with ATF6, SQSTM1, P4HB, AKT1, and CALR in most cancers. In response to ER stress, the transmembrane protein ATF6 acts as a transcription factor [44]. Overexpression of ATF6 and HSPA5 has been linked to poor prognosis in several tumor types, such as breast cancer [45], hepatocellular carcinoma [46], and colorectal cancer [47], according to various studies. Furthermore, the ATF6-HSPA5 interaction has been implicated in therapy resistance, as the upregulation of ATF6 and HSPA5 has been associated with resistance to chemotherapy [35]. Previous studies have shown that SQSTM1 is regulated by HSPA5 in different cancer types, such as breast and colorectal cancers [48]. Research suggests that SQSTM1 directly binds to HSPA5, which is upregulated during ER stress. This binding promotes activation of the UPR and autophagy, which can contribute to therapy resistance [48]. Evidence indicates that CALR can bind directly to HSPA5, promoting the UPR [49]. This interaction is implicated in the modulation of apoptotic resistance in cancer cells. The role of the CALR-HSPA5 interaction in tumors is multifaceted. This interaction can promote cell survival and resistance to therapy by activating pro-survival pathways [50]. However, this interaction can also induce cell apoptosis via the PERK-eIF2α-

CHOP pathway, which is part of the UPR and can lead to apoptosis [49]. Additionally, through enrichment analysis based on KEGG and GO, we discovered that HSPA5 can potentially activate the chaperone-mediated autophagy pathway, promote unfolded protein binding, or alter tumor progression by altering the ER protein-containing complex. Targeting these pathways and processes may offer potential strategies for inhibiting tumor progression. Thus, we found that HSPA5 may function as an oncogene in human cancers. However, experimental validation is necessary to strengthen the reliability of this hypothesis.

CAFs are essential for several biological processes related to cancer, including tumor development, angiogenesis, and immune homeostasis imbalance [51, 52]. They release growth factors, cytokines, and extracellular matrix (ECM) substances that assist tumor invasion and metastasis by promoting cancer cell survival and proliferation, stimulating angiogenesis, and altering the ECM [53]. Additionally, CAFs can modulate the immune response within the tumor microenvironment (TME), promoting an immunosuppressive environment that favors tumor progression [54]. In our study, most algorithms predicted that high HSPA5 expression would positively correlate with infiltration levels in 23 different cancers, including ACC, BLCA, CECS, COAD, ESCA, and GBM. Recent studies have highlighted the functional heterogeneity of CAFs, suggesting that different CAF subpopulations have distinct effects on cancer progression. CAF subsets have been identified based on the expression of certain markers and functional traits such as the capacity to stimulate angiogenesis and inhibit immune function [55]. In the TME, CD8+ T cells are often in a state of exhaustion [56]. This study also demonstrated that in THYM, HNSC, and GBM, HSPA5 expression is positively associated with CAFs but negatively correlated with the degree of CD8+ T cell infiltration (Supplementary Figure 3). These findings suggest that HSPA5-targeted therapies may be effective against these tumors when used in conjunction with immunotherapy. In general, our findings provide valuable insights into the role of CAFs in diverse tumors, potentially facilitating future investigations of CAFs and the TME. Yoshihara et al. developed a computational method called ESTIMATE [26] that generates three scores: immune, stromal, and estimated. We found a positive correlation between HSPA5 expression and the BLCA, COAD + READ, DLBC, GBM + LGG, KIPAN, and LGG scores. However, negative correlations were observed for ALL, LUAD, PRAD, STAD, and STES. Therefore, HSPA5-targeted therapy should be tailored to specific tumor types rather than adopting a "one-size-fits-all" approach.

Immune checkpoints are regulatory molecules on immune cells, particularly T cells, which help maintain self-tolerance and prevent autoimmunity by modulating the immune response [57]. Cancer cells exploit these checkpoints to evade immune recognition and destruction. Immune checkpoint inhibitors (ICIs) are monoclonal antibodies that target immune checkpoint molecules such as CTLA4, PD-1, and its ligand PD-L1, effectively releasing the immune system's brakes and promoting antitumor immunological responses [58, 59]. This study found a significant association between HSPA5 expression and PD-L1, PD-1, and CTLA-4 targets in a variety of tumors, including VM, BRCA, LIHC OV, BLCA, KIPAN, and READ. This finding raises the possibility that HSPA5 may act as a new biomarker for PD-L1, PD-1, and CTLA-4 in these tumors. To verify this, specimens from patients with breast cancer and hepatocellular carcinoma were analyzed. In the breast cancer and hepatocellular carcinoma tissues, large numbers of cancer cells exhibited high expression of HSPA5 and PD-L1, forming a statistically significant difference compared with the control group. However, in gastric cancer patients, the difference between HSPA5 and PD-L1 expression levels was not significant. We further conducted a series of in vitro experiments to investigate the effects of HSPA5 on tumor cells. Considering the abundant literature on the role of HSPA5 in breast cancer, such as Chen reported inhibition of HSPA5 suppresses cell migration and invasion in triple-negative breast cancer [11] and Katherine L Cook suggested HSPA5 was found to impact many different cellular processes that affect breast cancer survival [60]. We chose the human hepatocellular carcinoma cell line Hep3B for validation. We found that knocking down HSPA5 reduced the proliferation, invasion, and migration capabilities of Hep3B cells in vitro. Similar findings have also been reported [61], but the underlying mechanisms need further experimental confirmation.

Our study presents the findings of a comprehensive cancer analysis of HSPA5 expression. This investigation is the first to combine HSPA5 expression, prognosis, KEGG pathway and GO enrichment analyses, immune score, stromal score, estimate score, CAFs, and immune checkpoints. These findings were validated using patient specimens. In summary, our results demonstrate that HSPA5 functions as an oncogene in most of the examined cancers. Overexpression of HSPA5 can contribute to poor prognosis in various types of cancer, and sheds fresh light on the prognostic role of HSPA5 and its possible participation in tumor development.

Acknowledgements

The results presented in this study are partially derived from data generated by the TCGA Research Network (https://www.cancer.gov/tcga), and HPA database (https://www.proteinatlas.org/). This study was supported by the National Natural Science Foundation of China (No. 81871577, No. 82272508, No. 82072194 and No. 81901978).

Disclosure of conflict of interest

None.

Address correspondence to: Drs. Panfeng Wu and Xiaoyang Pang, Department of Orthopedics, Xiangya Hospital, Central South University, No. 87 Xiangya Road, Changsha 410008, Hunan, China. E-mail: wupanfeng@csu.edu.cn (PFW); xiaoyangpang@csu.edu.cn (XYP)

References

[1] Lee AS. The ER chaperone and signaling regulator GRP78/BiP as a monitor of endoplasmic reticulum stress. Methods 2005; 35: 373-381.
[2] Schröder M and Kaufman RJ. The mammalian unfolded protein response. Annu Rev Biochem 2005; 74: 739-789.
[3] Kim SY, Kim HJ, Kim HJ, Kim DH, Han JH, Byeon HK, Lee K and Kim CH. HSPA5 negatively regulates lysosomal activity through ubiquitination of MUL1 in head and neck cancer. Autophagy 2018; 14: 385-403.
[4] Li M, Zhao X, Yong H, Xu J, Qu P, Qiao S, Hou P, Li Z, Chu S, Zheng J and Bai J. Transketolase promotes colorectal cancer metastasis through regulating AKT phosphorylation. Cell Death Dis 2022; 13: 99.
[5] Wang J, Lee J, Liem D and Ping P. HSPA5 gene encoding Hsp70 chaperone BiP in the endoplasmic reticulum. Gene 2017; 618: 14-23.
[6] Gonzalez-Gronow M, Gopal U, Austin RC and Pizzo SV. Glucose-regulated protein (GRP78) is an important cell surface receptor for viral invasion, cancers, and neurological disorders. IUBMB Life 2021; 73: 843-854.
[7] Gao F, Fan H, Xue L, Shou Z, Zhu F, Yu T, Chu S, Wei C, Liu C, Zuo D and Zuo D. HSPA5 inhibitor meliorate DSS-induced colitis through HSPA1A/CHIP. Dis Markers 2022; 2022: 7115181.
[8] Kamath A, Joseph AM, Gupta K, Behera D, Jaiswal A, Dewan R and Rajala MS. Proteomic analysis of HEK293 cells expressing non small cell lung carcinoma associated epidermal growth factor receptor variants reveals induction of heat shock response. Exp Hematol Oncol 2015; 4: 16.
[9] Du T, Li H, Fan Y, Yuan L, Guo X, Zhu Q, Yao Y, Li X, Liu C, Yu X, Liu Z, Cui CP, Han C and Zhang L. The deubiquitylase OTUD3 stabilizes GRP78 and promotes lung tumorigenesis. Nat Commun 2019; 10: 2914.
[10] Chang YW, Tseng CF, Wang MY, Chang WC, Lee CC, Chen LT, Hung MC and Su JL. Deacetylation of HSPA5 by HDAC6 leads to GP78-mediated HSPA5 ubiquitination at K447 and suppresses metastasis of breast cancer. Oncogene 2016; 35: 1517-1528.
[11] Chen HA, Chang YW, Tseng CF, Chiu CF, Hong CC, Wang W, Wang MY, Hsiao M, Ma JT, Chen CH, Jiang SS, Wu CH, Hung MC, Huang MT and Su JL. E1A-mediated inhibition of HSPA5 suppresses cell migration and invasion in triple-negative breast cancer. Ann Surg Oncol 2015; 22: 889-898.
[12] Wang B, Lan T, Xiao H, Chen ZH, Wei C, Chen LF, Guan JF, Yuan RF, Yu X, Hu ZG, Wu HJ, Dai Z and Wang K. The expression profiles and prognostic values of HSP70s in hepatocellular carcinoma. Cancer Cell Int 2021; 21: 286.
[13] Aran G, Sanjurjo L, Bárcena C, Simon-Coma M, Téllez É, Vázquez-Vitali M, Garrido M, Guerra L, Díaz E, Ojanguren I, Elortza F, Planas R, Sala M, Armengol C and Sarrias MR. CD5L is upregulated in hepatocellular carcinoma and promotes liver cancer cell proliferation and antiapoptotic responses by binding to HSPA5 (GRP78). FASEB J 2018; 32: 3878-3891.
[14] Yang Z, Zhuang L, Szatmary P, Wen L, Sun H, Lu Y, Xu Q and Chen X. Upregulation of heat shock proteins (HSPA12A, HSP90B1, HSPA4, HSPA5 and HSPA6) in tumour tissues is associated with poor outcomes from HBV-related early-stage hepatocellular carcinoma. Int J Med Sci 2015; 12: 256-263.

[15] Jiang B, Zhang R, Zhang J, Hou Y, Chen X, Zhou M, Tian X, Hao C, Fan K and Yan X. GRP78-targeted ferritin nanocaged ultra-high dose of doxorubicin for hepatocellular carcinoma therapy. Theranostics 2019; 9: 2167-2182.
[16] Zhang T, Li J, Yang M, Ma X, Wang Z, Ma X, Sun M, Sun W, Xu J, Hua Y and Cai Z. CDK7/GRP78 signaling axis contributes to tumor growth and metastasis in osteosarcoma. Oncogene 2022; 41: 4524-4536.
[17] Tang X, Luo L, Li Y, Wu H, Hu Q, Yue H, He X, Zou J and Min S. Therapeutic potential of targeting HSPA5 through dual regulation of two candidate prognostic biomarkers ANXA1 and PSAT1 in osteosarcoma. Aging (Albany NY) 2020; 13: 1212-1235.
[18] Notaro A, Sabella S, Pellerito O, Di Fiore R, De Blasio A, Vento R, Calvaruso G and Giuliano M. Involvement of PAR-4 in cannabinoid-dependent sensitization of osteosarcoma cells to TRAIL-induced apoptosis. Int J Biol Sci 2014; 10: 466-478.
[19] Luo J, Xia Y, Yin Y, Luo J, Liu M, Zhang H, Zhang C, Zhao Y, Yang L and Kong L. ATF4 destabilizes RET through nonclassical GRP78 inhibition to enhance chemosensitivity to bortezomib in human osteosarcoma. Theranostics 2019; 9: 6334-6353.
[20] Cerami E, Gao J, Dogrusoz U, Gross BE, Sumer SO, Aksoy BA, Jacobsen A, Byrne CJ, Heuer ML, Larsson E, Antipin Y, Reva B, Goldberg AP, Sander C and Schultz N. The cBio cancer genomics portal: an open platform for exploring multidimensional cancer genomics data. Cancer Discov 2012; 2: 401-404.
[21] Li T, Fu J, Zeng Z, Cohen D, Li J, Chen Q, Li B and Liu XS. TIMER2.0 for analysis of tumor-infiltrating immune cells. Nucleic Acids Res 2020; 48: W509-W514.
[22] ICGC/TCGA Pan-Cancer Analysis of Whole Genomes Consortium. Pan-cancer analysis of whole genomes. Nature 2020; 578: 82-93.
[23] Clarke C, Madden SF, Doolan P, Aherne ST, Joyce H, O'Driscoll L, Gallagher WM, Hennessy BT, Moriarty M, Crown J, Kennedy S and Clynes M. Correlating transcriptional networks to breast cancer survival: a large-scale coexpression analysis. Carcinogenesis 2013; 34: 2300-2308.
[24] Chen F, Chandrashekar DS, Varambally S and Creighton CJ. Pan-cancer molecular subtypes revealed by mass-spectrometry-based proteomic characterization of more than 500 human cancers. Nat Commun 2019; 10: 5679.
[25] Liu J, Lichtenberg T, Hoadley KA, Poisson LM, Lazar AJ, Cherniack AD, Kovatich AJ, Benz CC, Levine DA, Lee AV, Omberg L, Wolf DM, Shriver CD and Thorsson V; Cancer Genome Atlas Research Network; Hu H. An integrated TCGA pan-cancer clinical data resource to drive high-quality survival outcome analytics. Cell 2018; 173: 400-416, e11.
[26] Yoshihara K, Shahmoradgoli M, Martínez E, Vegesna R, Kim H, Torres-Garcia W, Treviño V, Shen H, Laird PW, Levine DA, Carter SL, Getz G, Stemke-Hale K, Mills GB and Verhaak RG. Inferring tumour purity and stromal and immune cell admixture from expression data. Nat Commun 2013; 4: 2612.
[27] Nakamura Y, Tanaka F, Haraguchi N, Mimori K, Matsumoto T, Inoue H, Yanaga K and Mori M. Clinicopathological and biological significance of mitotic centromere-associated kinesin overexpression in human gastric cancer. Br J Cancer 2007; 97: 543-549.
[28] Wu C, Gong S, Duan Y, Deng C, Kallendrusch S, Berninghausen L, Osterhoff G and Schopow N. A tumor microenvironment-based prognostic index for osteosarcoma. J Biomed Sci 2023; 30: 23.
[29] Fu Y and Lee AS. Glucose regulated proteins in cancer progression, drug resistance and immunotherapy. Cancer Biol Ther 2006; 5: 741-744.
[30] Li Z, Wang Y, Newton IP, Zhang L, Ji P and Li Z. GRP78 is implicated in the modulation of tumor aerobic glycolysis by promoting autophagic degradation of IKKβ. Cell Signal 2015; 27: 1237-1245.
[31] Luo B and Lee AS. The critical roles of endoplasmic reticulum chaperones and unfolded protein response in tumorigenesis and anticancer therapies. Oncogene 2013; 32: 805-818.
[32] Guan Y, Zhu X, Liang J, Wei M, Huang S and Pan X. Upregulation of HSPA1A/HSPA1B/HSPA7 and downregulation of HSPA9 were related to poor survival in colon cancer. Front Oncol 2021; 11: 749673.
[33] Dong D, Stapleton C, Luo B, Xiong S, Ye W, Zhang Y, Jhaveri N, Zhu G, Ye R, Liu Z, Bruhn KW, Craft N, Groshen S, Hofman FM and Lee AS. A critical role for GRP78/BiP in the tumor microenvironment for neovascularization during tumor growth and metastasis. Cancer Res 2011; 71: 2848-2857.
[34] Kapoor V, Dadey DY, Nguyen K, Wildman SA, Hoye K, Khudanyan A, Bandara N, Rogers BE, Thotala D and Hallahan DE. Tumor-specific binding of radiolabeled PEGylated GIRLRG peptide: a novel agent for targeting cancers. J Nucl Med 2016; 57: 1991-1997.
[35] Pfaffenbach KT and Lee AS. The critical role of GRP78 in physiologic and pathologic stress. Curr Opin Cell Biol 2011; 23: 150-156.
[36] Yang Y, Hu H, Chen L, Zhang H and Yang J. A new survival model based on ferroptosis-related genes (FRGS) for prognostic prediction in

bladder cancer. Actas Urol Esp (Engl Ed) 2022; 46: 494-503.
[37] Samanta S, Yang S, Debnath B, Xue D, Kuang Y, Ramkumar K, Lee AS, Ljungman M and Neamati N. The hydroxyquinoline analogue YUM70 inhibits GRP78 to induce ER stress-mediated apoptosis in pancreatic cancer. Cancer Res 2021; 81: 1883-1895.
[38] Kabakov AE and Gabai VL. HSP70s in breast cancer: promoters of tumorigenesis and potential targets/tools for therapy. Cells 2021; 10: 3446.
[39] Cerezo M and Rocchi S. New anti-cancer molecules targeting HSPA5/BIP to induce endoplasmic reticulum stress, autophagy and apoptosis. Autophagy 2017; 13: 216-217.
[40] Ermakova SP, Kang BS, Choi BY, Choi HS, Schuster TF, Ma WY, Bode AM and Dong Z. (-)-Epigallocatechin gallate overcomes resistance to etoposide-induced cell death by targeting the molecular chaperone glucose-regulated protein 78. Cancer Res 2006; 66: 9260-9269.
[41] Lee JH, Yoon YM and Lee SH. GRP78 regulates apoptosis, cell survival and proliferation in 5-fluorouracil-resistant SNUC5 colon cancer cells. Anticancer Res 2017; 37: 4943-4951.
[42] Tsimberidou AM, Hong DS, Fu S, Karp DD, Piha-Paul S, Kies MS, Ravi V, Subbiah V, Patel SM, Tu SM, Janku F, Heymach J, Johnson A, Cartwright C, Zhao L, Zhang J, Berry DA, Vining DJ, Futreal A, Miller VA and Meric-Bernstam F. Precision medicine: preliminary results from the initiative for molecular profiling and advanced cancer therapy 2 (IMPACT2) study. NPJ Precis Oncol 2021; 5: 21.
[43] Cifaldi C, Rivalta B, Amodio D, Mattia A, Pacillo L, Di Cesare S, Chiriaco M, Ursu GM, Cotugno N, Giancotta C, Manno EC, Santilli V, Zangari P, Federica G, Palumbo G, Merli P, Palma P, Rossi P, Di Matteo G, Locatelli F, Finocchi A and Cancrini C. Clinical, immunological, and molecular variability of RAG deficiency: a retrospective analysis of 22 RAG patients. J Clin Immunol 2022; 42: 130-145.
[44] Yoshida H, Matsui T, Yamamoto A, Okada T and Mori K. XBP1 mRNA is induced by ATF6 and spliced by IRE1 in response to ER stress to produce a highly active transcription factor. Cell 2001; 107: 881-891.
[45] González-Ortiz A, Pulido-Capiz A, Castañeda-Sánchez CY, Ibarra-López E, Galindo-Hernández O, Calderón-Fernández MA, López-Cossio LY, Díaz-Molina R, Chimal-Vega B, Serafín-Higuera N, Córdova-Guerrero I and García-González V. eIF4A/PDCD4 pathway, a factor for doxorubicin chemoresistance in a triple-negative breast cancer cell model. Cells 2022; 11: 4069.
[46] Shuda M, Kondoh N, Imazeki N, Tanaka K, Okada T, Mori K, Hada A, Arai M, Wakatsuki T, Matsubara O, Yamamoto N and Yamamoto M. Activation of the ATF6, XBP1 and grp78 genes in human hepatocellular carcinoma: a possible involvement of the ER stress pathway in hepatocarcinogenesis. J Hepatol 2003; 38: 605-614.
[47] Lavoie S and Garrett WS. The unfolding story of ATF6, microbial dysbiosis, and colorectal cancer. Gastroenterology 2018; 155: 1309-1311.
[48] Wang Y, Xiong H, Liu D, Hill C, Ertay A, Li J, Zou Y, Miller P, White E, Downward J, Goldin RD, Yuan X and Lu X. Autophagy inhibition specifically promotes epithelial-mesenchymal transition and invasion in RAS-mutated cancer cells. Autophagy 2019; 15: 886-899.
[49] Kepp O, Senovilla L, Vitale I, Vacchelli E, Adjemian S, Agostinis P, Apetoh L, Aranda F, Barnaba V, Bloy N, Bracci L, Breckpot K, Brough D, Buqué A, Castro MG, Cirone M, Colombo MI, Cremer I, Demaria S, Dini L, Eliopoulos AG, Faggioni A, Formenti SC, Fučíková J, Gabriele L, Gaipl US, Galon J, Garg A, Ghiringhelli F, Giese NA, Guo ZS, Hemminki A, Herrmann M, Hodge JW, Holdenrieder S, Honeychurch J, Hu HM, Huang X, Illidge TM, Kono K, Korbelik M, Krysko DV, Loi S, Lowenstein PR, Lugli E, Ma Y, Madeo F, Manfredi AA, Martins I, Mavilio D, Menger L, Merendino N, Michaud M, Mignot G, Mossman KL, Multhoff G, Oehler R, Palombo F, Panaretakis T, Pol J, Proietti E, Ricci JE, Riganti C, Rovere-Querini P, Rubartelli A, Sistigu A, Smyth MJ, Sonnemann J, Spisek R, Stagg J, Sukkurwala AQ, Tartour E, Thorburn A, Thorne SH, Vandenabeele P, Velotti F, Workenhe ST, Yang H, Zong WX, Zitvogel L, Kroemer G and Galluzzi L. Consensus guidelines for the detection of immunogenic cell death. Oncoimmunology 2014; 3: e955691.
[50] Chou HC, Chen JY, Lin DY, Wen YF, Lin CC, Lin SH, Lin CH, Chung TW, Liao EC, Chen YJ, Wei YS, Tsai YT and Chan HL. Identification of up- and down-regulated proteins in pemetrexed-resistant human lung adenocarcinoma: flavin reductase and calreticulin play key roles in the development of pemetrexed-associated resistance. J Proteome Res 2015; 14: 4907-4920.
[51] Öhlund D, Elyada E and Tuveson D. Fibroblast heterogeneity in the cancer wound. J Exp Med 2014; 211: 1503-1523.
[52] Biffi G and Tuveson DA. Diversity and biology of cancer-associated fibroblasts. Physiol Rev 2021; 101: 147-176.
[53] Kalluri R. The biology and function of fibroblasts in cancer. Nat Rev Cancer 2016; 16: 582-598.
[54] Chen X and Song E. Turning foes to friends: targeting cancer-associated fibroblasts. Nat Rev Drug Discov 2019; 18: 99-115.

[55] Sahai E, Astsaturov I, Cukierman E, DeNardo DG, Egeblad M, Evans RM, Fearon D, Greten FR, Hingorani SR, Hunter T, Hynes RO, Jain RK, Janowitz T, Jorgensen C, Kimmelman AC, Kolonin MG, Maki RG, Powers RS, Puré E, Ramirez DC, Scherz-Shouval R, Sherman MH, Stewart S, Tlsty TD, Tuveson DA, Watt FM, Weaver V, Weeraratna AT and Werb Z. A framework for advancing our understanding of cancer-associated fibroblasts. Nat Rev Cancer 2020; 20: 174-186.

[56] Zhang L and Romero P. Metabolic control of CD8+ T cell fate decisions and antitumor immunity. Trends Mol Med 2018; 24: 30-48.

[57] Mariathasan S, Turley SJ, Nickles D, Castiglioni A, Yuen K, Wang Y, Kadel EE III, Koeppen H, Astarita JL, Cubas R, Jhunjhunwala S, Banchereau R, Yang Y, Guan Y, Chalouni C, Ziai J, Şenbabaoğlu Y, Santoro S, Sheinson D, Hung J, Giltnane JM, Pierce AA, Mesh K, Lianoglou S, Riegler J, Carano RAD, Eriksson P, Höglund M, Somarriba L, Halligan DL, van der Heijden MS, Loriot Y, Rosenberg JE, Fong L, Mellman I, Chen DS, Green M, Derleth C, Fine GD, Hegde PS, Bourgon R and Powles T. TGFβ attenuates tumour response to PD-L1 blockade by contributing to exclusion of T cells. Nature 2018; 554: 544-548.

[58] Dai X, Bu X, Gao Y, Guo J, Hu J, Jiang C, Zhang Z, Xu K, Duan J, He S, Zhang J, Wan L, Liu T, Zhou X, Hung MC, Freeman GJ and Wei W. Energy status dictates PD-L1 protein abundance and anti-tumor immunity to enable checkpoint blockade. Mol Cell 2021; 81: 2317-2331, e6.

[59] Schoenfeld AJ, Rizvi H, Bandlamudi C, Sauter JL, Travis WD, Rekhtman N, Plodkowski AJ, Perez-Johnston R, Sawan P, Beras A, Egger JV, Ladanyi M, Arbour KC, Rudin CM, Riely GJ, Taylor BS, Donoghue MTA and Hellmann MD. Clinical and molecular correlates of PD-L1 expression in patients with lung adenocarcinomas. Ann Oncol 2020; 31: 599-608.

[60] Cook KL, Clarke PA and Clarke R. Targeting GRP78 and antiestrogen resistance in breast cancer. Future Med Chem 2013; 5: 1047-1057.

[61] Wu LF, Guo YT, Zhang QH, Xiang MQ, Deng W, Ye YQ, Pu ZJ, Feng JL and Huang GY. Enhanced antitumor effects of adenoviral-mediated siRNA against GRP78 gene on adenosine-induced apoptosis in human hepatoma HepG2 cells. Int J Mol Sci 2014; 15: 525-544.

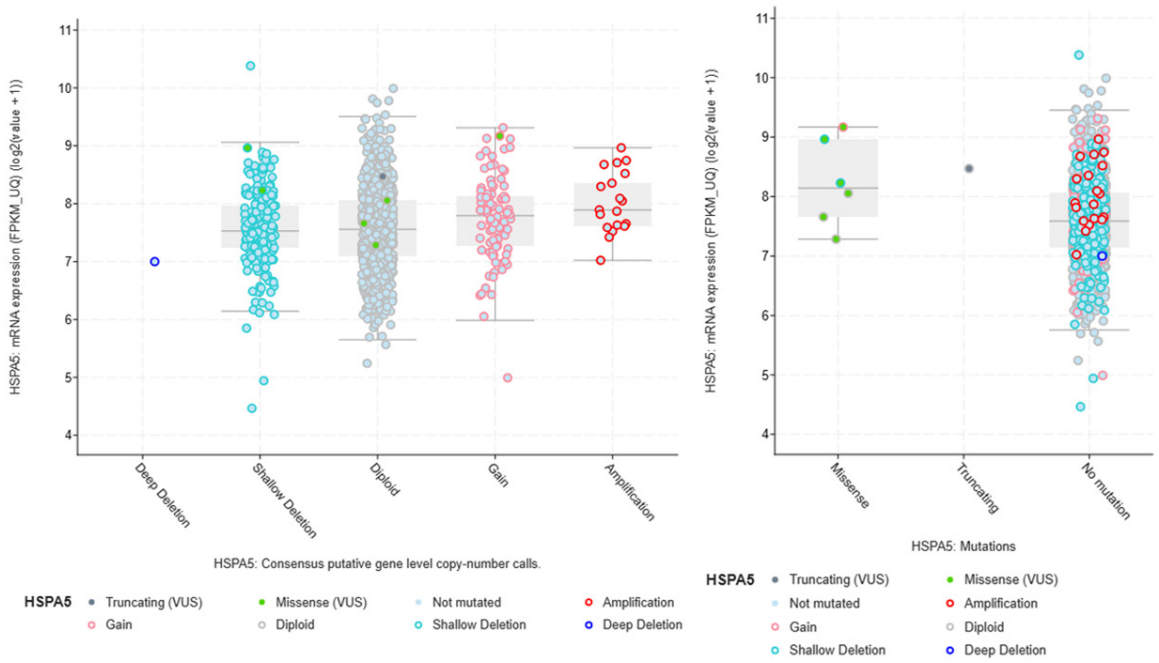

Supplementary Figure 1. HSPA5 transcriptional expression in the TCGA cohort characterized by diverse copy numbers (Left) and mutations (Right).

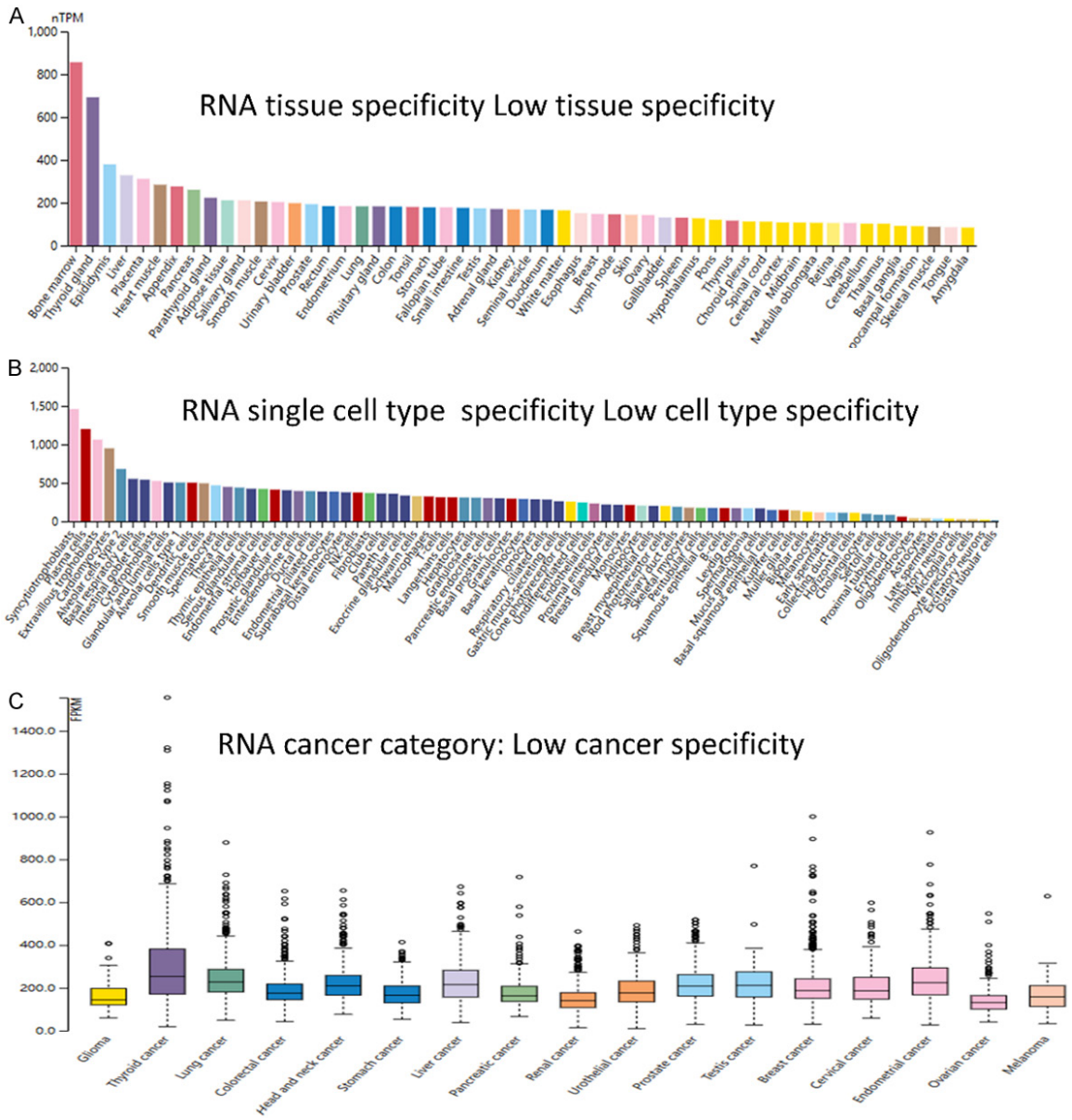

Supplementary Figure 2. Expression levels of HSPA5 in different normal tissues, single cell types, and tumor tissues. A. HSPA5 gene in various normal tissues using the HPA, GTEx, and FANTOM5 consensus datasets. B. HSPA5 gene in different single cell types. C. Expression of the HSPA5 gene in various tumors.

Supplementary Table 1. The HSPA5-correlated genes and HSPA5-interacted proteins

100 correlated genes	50 interacted proteins
HSP90B1	A2M
MANF	AKT1
PDIA3	ATF4
PDIA4	ATF6
PDIA6	BAG1
HYOU1	BAG2
RP11-334L9.1	BAG3
CALR	CALR

MESDC2
ERP44
DNAJC3
SURF4
MAGT1
CRELD2
RPN1
STT3A
ALG2
ERLEC1
RAB1A
SEC61A1
DDOST
SLC33A1
NUS1
SEC24D
DERL2
TMED10
GANAB
ARCN1
COPB2
RPN2
TMED9
SDF2L1
TMED2
USO1
MINA
ISY1-RAB43
PPIB
LMAN1
TVP23B
PDIA3P1
SLC39A7
MCFD2
OSTC
EIF2AK3
TMED7
CDC27
SRP19
TCTN3
MARVELD2
PCYOX1
ACBD3
YME1L1
SSR3
PRRC1
TMEM214
ARF4
APMAP

CANX
CASP7
CDH13
CLU
DNAJB1
DNAJB11
DNAJB6
DNAJC1
DNAJC10
DNAJC2
DNAJC3
DNAJC7
EGFR
EIF2AK3
ERN1
HSP90AA1
HSP90B1
HSPD1
HSPH1
HYOU1
IGFBP3
MANF
OS9
P4HB
PAWR
PDIA3
PDIA4
PDIA6
PLG
PPIB
PRNP
SEC13
SEC61A1
SEC63
SERPINA12
SIGMAR1
SIL1
SNCA
SOD1
SQSTM1
TDGF1
XBP1

MED8
SEC23B
GPR107
SLC30A5
P4HB
YIPF4
DNAJB11
SPCS3
LMAN2
CANX
RRBP1
TPMT
UGGT1
DCTD
COPB1
SELENOF
SRPRB
VEZT
TOR1A
GOLGA5
ARL1
TMEM50B
GFPT1
RAD23B
ZBTB2
TM9SF1
SSR1
SEC31A
SDF4
TMED4
MMADHC
ARF1
SPTLC1
EXT2
KDELR2
DNAJC10
TG
DDX31
CREB3L2
TVP23C-CDRT4
C9orf64
GMPPB
TXNL1

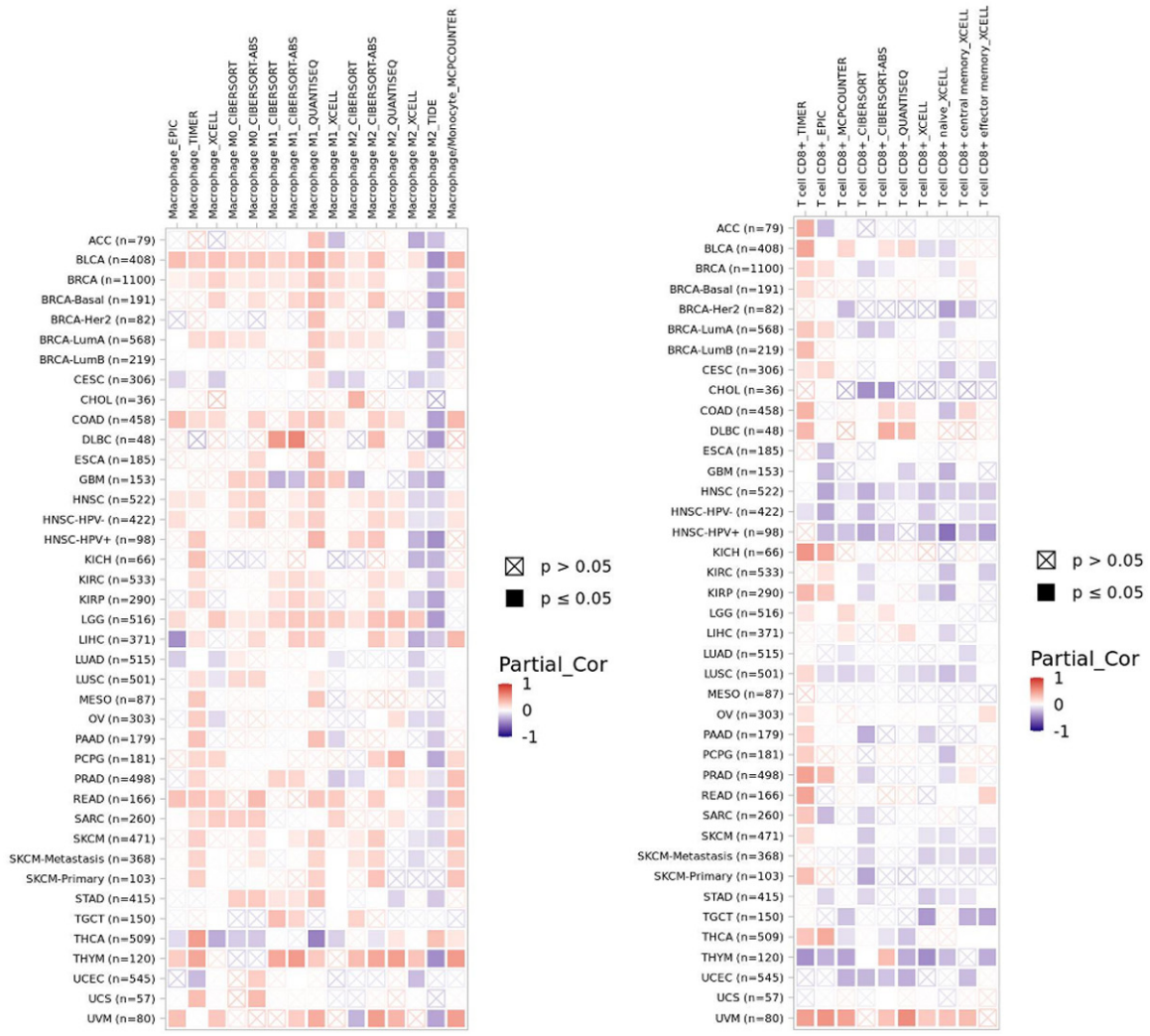

Supplementary Figure 3. HSPA5 expression associated with various immune cells in various tumor types. *P < 0.05.

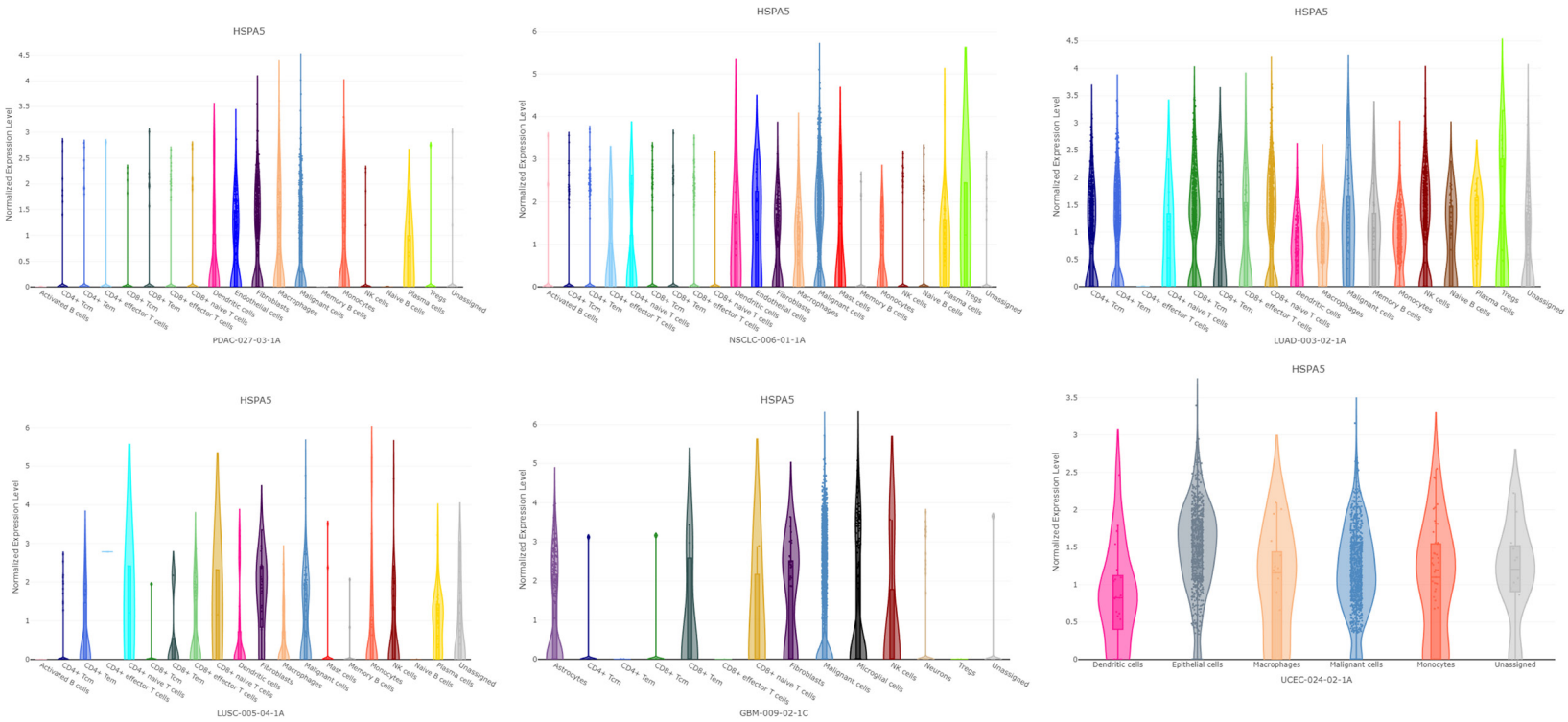

Supplementary Figure 4. Analysis of HSPA5 expression in cancer from single-cell data: Map of single-cell expression. HSPA5 expression is observed in malignant cells and various immune cells.